# Long range disorder and Anderson transition in systems with chiral symmetry

Antonio M. García-García
*Laboratoire de Physique Théorique et Modèles Statistiques, Bât. 100, Université de Paris-Sud, 91405 Orsay Cedex, France*

Kazutaka Takahashi
*Theoretische Physik III, Ruhr-Universität Bochum, 44780 Bochum, Germany*

(Dated: February 2, 2008)

We study the spectral properties of a chiral random banded matrix (chRBM) with elements decaying as a power-law $\mathcal{H}_{ij} \sim |i-j|^{-\alpha}$. This model is equivalent to a chiral 1D Anderson Hamiltonian with long range power-law hopping. In the weak disorder limit we obtain explicit nonperturbative analytical results for the density of states (DoS) and the two-level correlation function (TLCF) by mapping the chRBM onto a nonlinear $\sigma$ model. We also put forward, by exploiting the relation between the chRBM at $\alpha = 1$ and a generalized chiral random matrix model, an exact expression for the above correlation functions. We give compelling analytical and numerical evidence that for this value the chRBM reproduces all the features of an Anderson transition. Finally we discuss possible applications of our results to quantum chromodynamics (QCD).

PACS numbers: 72.15.Rn, 71.30.+h, 05.45.Df, 05.40.-a

## I. INTRODUCTION

The spectral properties of a disordered system, namely, a noninteracting particle in a random potential, are strongly affected by the global symmetries of the Hamiltonian. In the ergodic/metallic regime, the spectral correlations of generic quantum complex systems with translational invariant spectrum fall in three universality classes ('standard' from now on) attending to time reversal and spin symmetries. The simplest representative of each universality class corresponds to an ensemble of matrices with the appropriate symmetry and random Gaussian entries. Typical properties of the spectral fluctuations of these matrices include level repulsion and spectral rigidity. In the literature they are usually referred as Wigner-Dyson (WD) statistics [1].

In recent years new ('nonstandard' from now on) universality classes have been put forward by relaxing the translational invariance condition [2, 3, 4, 5]. These classes are related to additional symmetries of the system. For instance, for (random) matrices with block structure

$$\mathcal{H} = \begin{pmatrix} 0 & C \\ C^\dagger & 0 \end{pmatrix}, \tag{1}$$

where $C$ is a general $n \times (n+\nu)$ real, complex or quaternionic matrix, the eigenvalues come in pairs of $\pm\epsilon_i$ or are zero. This discrete symmetry is usually called chiral and induces an additional level repulsion around zero which results in different spectral correlations for eigenvalues near zero (the origin) and away from zero (the bulk). In the bulk the spectral correlations are not affected by the block structure and WD statistics applies.

The motivation to study these nonstandard symmetry classes comes from different branches of theoretical physics. In the context of QCD, the Dirac operator in a chiral basis has a similar block structure. It turns out that in the infrared (ergodic) limit, the eigenvalue correlations of this operator do not depend on the dynamics details of the QCD Lagrangian but only on the global (chiral) symmetries of the QCD partition function [2]. Thus random matrices with the correct chiral symmetry of QCD (termed chiral random matrices) [6] accurately describe the spectral properties of the QCD Dirac operator up to some scale known as the Thouless energy [7]. As in the standard case, depending on the invariance under time reversal symmetry and spin, there exist three chiral random matrix ensembles. In the context of QCD each universality class is related to both the number of colors and the fermionic representation considered.

Another interesting problem that falls beyond the standard classification is that of the spectral correlations of a mesoscopic disordered system composed of both normal conducting and superconducting parts. In this case, in an appropriate basis, the mean field Bogouliobov-de Gennes Hamiltonian can be expressed as

$$\mathcal{H} = \begin{pmatrix} h & \Delta \\ -\Delta^* & -h^T \end{pmatrix} \tag{2}$$

where $\Delta$ is a matrix representing the pairing field and $h$ is a matrix representation of the disordered free Hamiltonian.

The Hamiltonian $\mathcal{H}$ can be effectively modeled as a random matrix provided that the phase shift due to reflection in the NS interphase vanishes on average [5]. In this situation the gap at the chemical potential disappears and thus

pseudo particle excitations appear at arbitrarily low energies. The resulting spectral properties also fall apart from WD statistics. In this case four new universality classes are found attending to spin and time reversal symmetries. Other systems with similar nonstandard symmetries include random flux models [8] (here disorder is placed not in the site but in the link (bond disorder)) and bosons in random media [9].

As a general rule (valid for all standard and nonstandard symmetry classes), localization effects tend to gradually erase the impact of symmetries. However, the transition to localization is not the same in both cases. In systems with nonstandard symmetries the localization properties are in general sensitive to details as the microscopic form of the random potential [10] or the number (odd or even) of lattice points considered [11]. In certain situations [12, 13, 14], for energies close to zero, the DoS diverges and eigenvectors remain delocalized even in the strong disorder regime in 1D or 2D. By contrast, in the standard case the spectral correlations are insensitive to the microscopic details of the dynamics provided that the disordered potential is short-range. The eigenstates of a free particle in a disordered medium in less than 3D are localized in the thermodynamic limit for any amount of disorder. In three and higher dimensions there exists a metal insulator transition (Anderson transition) for a critical amount of disorder.

For finite systems, the dimensionless conductance $g = E_c/\Delta$ ($E_c = \hbar/t_c$ is the Thouless energy, $t_c$ is the classical time to cross the sample diffusively, and $\Delta$ is the quantum mean level spacing) is a useful magnitude to quantify the deviations from WD statistics due to wavefunction localization. We recall that WD statistics applies in the metallic/delocalized regime $g \to \infty$. Nonperturbative corrections due to a finite $g \gg 1$ (weak disorder) were recently evaluated by Andreev and Altshuler [15] by mapping the localization problem onto a supersymmetric nonlinear $\sigma$ model [16]. They managed to express the TLCF in terms of the spectral determinant of the classical diffusion operator. As disorder strength increases, localization becomes dominant $g \sim 1$ and eventually the system undergoes a metal insulator transition. Unfortunately the above analytical tools cease to be applicable in this region. Numerical simulations of 3D short range Anderson models suggest that, at the Anderson transition, the wavefunction moments $P_q$ present anomalous scaling with respect to the sample size $L$, $P_q = \int d^d r |\psi(\mathbf{r})|^{2q} \propto L^{-D_q(q-1)}$, where $D_q$ is a set of exponents describing the transition [17]. Wavefunctions with such a nontrivial scaling are said to be multifractal (for a review see Ref.[18]). Spectral fluctuations at the Anderson transition (commonly referred as 'critical statistics' [19]) are intermediate between WD and Poisson statistics. Typical features include: scale invariant spectrum [20], level repulsion, and sub-Poisson number variance [21]. Different generalized random matrix model (gRMM) have been successfully employed to describe critical statistics [22, 23].

The study of these gRMM have shown that critical statistics and multifractal wavefunctions can be reproduced in the weak coupling regime $g \gg 1$ by allowing long range hopping in the original Anderson model. Actually power-law long range hopping, far from being a mathematical curiosity, appears in a broad range of systems: glasses with strong dipole interactions in real space [24], the evolution operator of Floquet systems [25] with a nonanalytical potential or in Hamiltonians leading to classical anomalous diffusion [26]. Although the introduction of long range hopping dates back to the famous Anderson's paper on localization [27], these models did not attract too much attention until the numerical work of Oono [28, 29] and the renormalization group (RG) treatment of Levitov [24] in the context of glassy systems. The main conclusion of these works was that power-law hopping may induce an Anderson transition in any dimension provided that the exponent of the hopping decay matches the dimension of the space.

A 1D version of this problem, a RBM with a power-law decay, was discussed in Ref.[23]. By mapping the problem onto a nonlinear $\sigma$ model with a nonlocal interaction, it was shown that for a $1/r$ band decay the eigenstates are multifractal and the spectral correlations resemble the ones at the Anderson transition. In this case the TLCF in the $g \gg 1$ limit is expressed in terms of the spectral determinant of a classical anomalous diffusion operator related to classical ballistic diffusion and $1/f$ noise [30]. Recent investigations [31] have further corroborated the close relation between this random banded matrix model and the Anderson model at the metal insulator transition.

In this work we want to study the interplay between long range disorder and chiral symmetry. Our main aim is to provide a detailed analytical account on how the transition to localization occurs in systems with chiral symmetry.

The organization of the paper is as follows. In Sec.II, we introduce a chRBM with power-law decay (equivalent to a 1D Anderson model with power-law hopping and chiral symmetry). After mapping it onto a nonlinear $\sigma$ model we investigate the localization properties by using the renormalization group formalism. In Sec.III, analytical results for both the DoS and the TLCF are obtained in different domains. We show for a special value of the power-law exponent ($\alpha = 1$) the resulting expression is greatly simplified. In Sec.IV, by exploiting the relation between the chRBM for $\alpha = 1$ and an exactly solvable random matrix model, we give an exact result for the DoS and the TLCF valid in the weak disorder regime. It is shown that the spectral correlations for this special value resemble those of a disordered system at the Anderson transition. We also conjecture an expression for the DoS and the TLCF for arbitrary power-law exponent. These analytical findings are supported by numerical results from direct diagonalization of the chRBM. Finally, in Sec.V, we discuss applications of our model in the context of QCD [2].

## II. THE CHIRAL RBM WITH POWER-LAW DISORDER

We study the spectral properties of an ensemble of Hermitian chRBM given by

$$\mathcal{H} = \begin{pmatrix} \omega_1 & \omega_2 \\ \omega_2 & -\omega_1 \end{pmatrix}, \tag{3}$$

where $\omega_{1,2}$ are $n \times n$ Hermitian matrices. This form is related to Eq.(1) at $\nu = 0$ by a unitary transformation. In this paper we restrict ourselves to the $\nu = 0$ case. The matrix elements $(\omega_{1,2})_{ij}$ are independently distributed complex Gaussian variables with zero mean and variance

$$\langle |(\omega_{1,2})_{ij}|^2 \rangle = a^2(r) = \frac{1}{1 + (r/r_0)^{2\alpha}}, \tag{4}$$

where $r_0$ and $\alpha$ are real parameters and $r = |i - j|$ is the spectral distance. The choice of complex matrix elements corresponds to a matrix model with unitary symmetry. Due to the chiral symmetry, the eigenvalues of Eq.(3) come in pairs of $\pm\epsilon_i$. This feature induces thus an additional level repulsion around zero and consequently the spectral correlations for eigenvalues near zero (the origin) and away from zero (the bulk) are essentially different. At the bulk the spectral correlations are not affected by the block structure and coincide with the nonchiral version of Eq.(3) which has been intensively studied in recent years [23, 31].

In this section we study the localization properties at the origin by mapping the chRBM (3) onto a supersymmetric nonlinear $\sigma$ model [16]. The above chRBM can also be interpreted as a 1D chiral Anderson model with long range disorder. In this context the parameter $r_0$ measures the amount of off-diagonal disorder. Thus the $r_0 \gg 1$ ($r_0 \ll 1$) limit corresponds with the weak (strong) disorder regime. In this paper, due to technical reasons (large-$r_0$ allows us to use the saddle-point approximation in the derivation of the nonlinear $\sigma$ model), we are focused on the weak disorder limit. Concerning the power-law exponent $\alpha$, we are mainly interested in the range $1/2 < \alpha \leq 3/2$. It is known that the spectral correlations for the nonchiral RBM case $\alpha \leq 1/2$ are well described by WD statistics [23]. We expect this holds also in the present chiral case and we do not consider it in this paper. On the other hand, as shown below, for $\alpha > 3/2$ our model is similar to a standard 1D short range chiral Anderson model recently investigated in Ref.[32].

### A. Supersymmetric nonlinear $\sigma$ model

We use the supersymmetry method [16] to derive the sigma model. We shall follow Efetov's notations and conventions. As usual, the first step is to express the correlation function as a ratio of two determinant. For the one point retarded Green function,

$$G^{(R)}(\epsilon) = \frac{1}{\epsilon^+ - \mathcal{H}} = \frac{1}{2} \frac{\partial}{\partial J} Z[J] \Big|_{J=0}, \tag{5}$$

where $\epsilon^+ = \epsilon + i\delta$ is the energy with small imaginary part and the generating function $Z[J]$ is given by

$$Z[J] = \frac{\det(\epsilon^+ - \mathcal{H} + J)}{\det(\epsilon^+ - \mathcal{H} - J)}. \tag{6}$$

The source field $J_{ij}$ is a $2n \times 2n$ complex matrix. The above ratio can be written as a Gaussian integral over a supervector with both fermionic and bosonic components as

$$Z[J] = \int \mathcal{D}(\psi, \bar{\psi}) \exp\left[ i\bar{\psi}(\epsilon^+ - \mathcal{H} + kJ)\psi \right], \tag{7}$$

where $k = \mathrm{diag}(1, -1)$ in superspace, $\psi$ is a $4n$-component supervector and $\bar{\psi} = \psi^\dagger$.

Following the standard method, we perform the spectral averaging over $\mathcal{H}$ and introduce the 4×4 supermatrix $Q$ using the Hubbard-Stratonovich transformation. After these steps are carried out, the generating function is given by

$$\langle Z[J] \rangle = \int \mathcal{D}Q \exp\left[ -\frac{A_0}{2} \sum_{i,j=1}^{n} (A^{-1})_{ij} \mathrm{str}\, Q_i Q_j + \mathrm{str}\, \ln\left( \epsilon^+ \Sigma_z + kJ\Sigma_z + i\sqrt{A_0} Q \right) \right], \tag{8}$$

where $A_{ij} = a^2(|i - j|)$, $A_0 = n^{-1} \sum_{i,j=1}^{n} A_{ij}$, $\Sigma_z$ is the Pauli matrix in chiral space and the $Q$-matrix verifies $\{Q, \Sigma_x\} = 0$. In the limit $A_0 \sim r_0 \gg 1$ the integral over $Q$ can be performed by the saddle-point method. It is

not hard to show that in this case the solution of the saddle point equation is $Q_i = \Sigma_z$ at $\epsilon = 0$. Consequently the saddle point manifold $Q^2 = 1$ is parametrized as $Q = T\Sigma_z\bar{T}$ where $T$ is the matrix with symmetry specified below and $\bar{T} = T^{-1}$. In addition to that, the massive mode changing the saddle point should also be integrated out. Unlike the standard case, the effect of these modes plays an important role in our case. The matrix $Q$ is thus parametrized as

$$Q_i = T_i(\Sigma_z + \delta Q_i)\bar{T}_i, \quad \delta Q_i = \delta q_i \Sigma_z, \tag{9}$$

where $\delta q_i$ is a $2\times2$ supermatrix. In order to proceed we first perform an expansion in powers of $\delta Q$ up to second order, and then integrate over it (it is just a Gaussian integration). After these manipulations we find $\langle Z[J]\rangle = \int \mathcal{D}Q \exp(-F)$ with

$$F = \frac{A_0}{2}\sum_{ij} R_{ij}\mathrm{str}\, Q_iQ_j - \frac{1}{4}\sum_{ij} R_{ij}\mathrm{str}\,\bar{T}_jT_i\Sigma_x\mathrm{str}\,\bar{T}_iT_j\Sigma_x + \frac{i\pi\epsilon}{2n\Delta}\sum_i \mathrm{str}\,\Sigma_zQ_i + \frac{i\pi}{2n\Delta}\sum_{ij}\mathrm{str}\, J_{ij}k\Sigma_zQ_j, \tag{10}$$

where $R_{ij} = (A^{-1})_{ij} - n^{-1}\delta_{ij}\sum_{kl}(A^{-1})_{kl}$, and $\Delta = \pi\sqrt{A_0}/2n$ is the inverse of the DoS (mean level spacing) at $\epsilon = 0$.

We remark that the above results can be applied to any $a(r)$ provided that $A_0$ is large enough. For technical details we refer to Ref.[32] where a $a(r)$ with exponential decay was considered. Compared with the sigma model for the nonchiral RBM, we found an additional contribution having the double-supertrace form (second term of Eq.(10)). This term was derived by integrating over the massive modes. We recall that in its derivation it was crucial that the massive modes were parametrized as in Eq.(9).

In order to proceed we have to make a gradient expansion of the kinetic term in Eq.(10). As in the standard case [23], this expansion depends on the value of $\alpha$. For $\alpha > 3/2$

$$\begin{aligned}\frac{A_0}{2}\sum_{ij} R_{ij}\mathrm{str}\, Q_iQ_j &\sim -\frac{A_0}{4}\sum_{ij}(i-j)^2R_{ij}\mathrm{str}\,(\nabla Q_i)^2 \\ &\sim -\frac{A_0^{(2)}}{4A_0}\int dx\mathrm{str}\,(\nabla Q(x))^2,\end{aligned} \tag{11}$$

where

$$\begin{aligned}A_0 &= 2\int_0^\infty dr\frac{1}{1+(r/r_0)^{2\alpha}} = 2r_0\frac{\frac{\pi}{2\alpha}}{\sin\frac{\pi}{2\alpha}},\\ -A_0^{(2)} &= 2\int_0^\infty dr\frac{r^2}{1+(r/r_0)^{2\alpha}} = 2r_0^3\frac{\frac{\pi}{2\alpha}}{\sin\frac{3\pi}{2\alpha}},\\ -\frac{A_0^{(2)}}{A_0} &= r_0^2\frac{\sin\frac{\pi}{2\alpha}}{\sin\frac{3\pi}{2\alpha}}.\end{aligned} \tag{12}$$

We see that the integral in $A_0^{(2)}$ is well-defined for $\alpha > 3/2$. After a similar expansion in the double trace term above, we find the normal diffusive $\sigma$ model for $\alpha > 3/2$

$$F = \frac{i\pi\epsilon}{2\Delta V}\int dx\mathrm{str}\,\Sigma_zQ(x) + \frac{1}{4b}\int dx\mathrm{str}\,(\nabla Q(x))^2 - \frac{1}{4c}\int dx\,(\mathrm{str}\,Q(x)\nabla Q(x)\Sigma_x)^2\,, \tag{13}$$

where for the sake of simplicity we have neglected the source term, and $V = n$ is the 'system volume'. The coupling constants $b$ and $c$ are given by

$$\frac{1}{b} = -\frac{A_0^{(2)}}{A_0} = r_0^2\frac{\sin\frac{\pi}{2\alpha}}{\sin\frac{3\pi}{2\alpha}}, \quad \frac{1}{c} = -\frac{A_0^{(2)}}{4A_0^2} = \frac{r_0}{8}\frac{\sin^2\frac{\pi}{2\alpha}}{\frac{\pi}{2\alpha}\sin\frac{3\pi}{2\alpha}}. \tag{14}$$

For $1/2 < \alpha \le 3/2$ the gradient expansion requires a special care since $A_0^{(2)}$ is not well-defined. Taking into account higher order terms in the gradient expansion (as in Ref.[23]), we find the following expression for $A_0^{(2)}$,

$$q^2\int_0^\infty dr\frac{r^2}{1+(r/r_0)^{2\alpha}} \to 2\int_0^\infty dr\frac{1-\cos qr}{1+(r/r_0)^{2\alpha}} \sim C_\alpha r_0^{2\alpha-1}|q|^{2\alpha-1}, \tag{15}$$

where $C_\alpha = 2\int_0^\infty dx(1-\cos x)/x^{2\alpha}$ is a numerical constant. With this substitution Eq.(10) for $1/2 < \alpha \leq 3/2$ is given by

$$\begin{aligned} F &= \frac{i\pi\epsilon}{2\Delta V}\int dx \mathrm{str}\,\Sigma_z Q(x) + \frac{1}{4b}\int \frac{dq}{2\pi}|q|^{2\alpha-1}\mathrm{str}\,Q(q)Q(-q) \\ &\quad -\frac{1}{4c}\int \frac{dq}{2\pi}\frac{dp}{2\pi}\frac{dp'}{2\pi}|q|^{2\alpha-1}\mathrm{str}\,Q(p+q)Q(-p)\Sigma_x \mathrm{str}\,Q(p'-q)Q(-p')\Sigma_x, \end{aligned} \tag{16}$$

where

$$\frac{1}{b} = \frac{2C_\alpha r_0^{2\alpha}}{A_0} = C_\alpha r_0^{2\alpha-1}\frac{\sin\frac{\pi}{2\alpha}}{\frac{\pi}{2\alpha}}, \quad \frac{1}{c} = \frac{C_\alpha r_0^{2\alpha}}{2A_0^2} = \frac{C_\alpha r_0^{2\alpha-2}}{8}\left(\frac{\sin\frac{\pi}{2\alpha}}{\frac{\pi}{2\alpha}}\right)^2. \tag{17}$$

In this case, unlike for $\alpha > 3/2$, the nonlinear $\sigma$ mode (16) corresponds with a process of anomalous diffusion. However, we note that the relation $1/b = 4A_0/c \sim r_0/c$ holds in both cases and $1/c \ll 1/b$. Thus the double trace term (last term of $F$) will not affect the spectral properties to leading order in $1/r_0$. Its role in the localization properties of the chRBM is discussed below.

### B. Renormalization group equations

By using the above nonlinear $\sigma$ model Eqs.(13) and (16), one can discuss the localization properties of our chRBM in the thermodynamic limit. This can be done by investigating the running of the coupling constants $b$ and $c$ under the RG flow. We compute the RG equations to leading order in $b$ and $b^2/c$. For the normal diffusive case, Eq.(13), the parameters $b$ and $b^2/c$ involve the following propagators

$$\Pi(q,\omega) = \frac{1}{q^2 - i\omega}, \quad \Pi_2(q,\omega) = q^2\Pi^2(q,\omega) \quad (\text{For } \alpha > 3/2), \tag{18}$$

respectively. On the other hand, in the anomalous diffusive case, Eq.(16), the propagators are given by

$$\Pi(q,\omega) = \frac{1}{|q|^{2\alpha-1} - i\omega}, \quad \Pi_2(q,\omega) = |q|^{2\alpha-1}\Pi^2(q,\omega) \quad (\text{For } 1/2 < \alpha \leq 3/2). \tag{19}$$

By observing the momentum integrations of the propagators

$$\int_{\Lambda/l}^{\Lambda}\frac{d^dq}{(2\pi)^d}\Pi(q,\omega) \sim \frac{1}{2\pi}\ln l, \quad \int_{\Lambda/l}^{\Lambda}\frac{d^dq}{(2\pi)^d}\Pi_2(q,\omega) \sim \frac{1}{2\pi}\ln l, \tag{20}$$

where $\Lambda$ is a cutoff and $l \sim n > 1$, we conclude that for normal diffusion the logarithmic dimension is $d = 2$. For anomalous diffusion, since our chRBM is in essence one dimensional, the logarithmic dimension corresponds to the case $\alpha = 1$ (generally, $d = 2\alpha - 1$). We note that it is a straightforward task to extend the derived $\sigma$ model for the chRBM to arbitrary dimension.

In the normal diffusive case, the perturbative calculation of the RG equations was first done in Ref.[12] by the method of the $\epsilon$-expansion. The RG equations are given by

$$\beta_b = -\frac{db}{d\mu} = \epsilon b, \quad \beta_c = -\frac{dc}{d\mu} = \epsilon c + \frac{1}{8\pi}c^2, \quad \zeta = \frac{1}{2\pi}\frac{b^2}{c}, \tag{21}$$

where $\mu = \ln l$ is the renormalization scale, $\beta_{b,c}$ are the beta functions for $b$ and $c$ and $\zeta$ is the wavefunction renormalization. The above equations are immediately applied to the anomalous case by replacing $\epsilon = d-2$ by $\epsilon = 1-(2\alpha-1)$. The RG equations are easily solved for arbitrary $\epsilon$ [12]. We see that, in the domain $\epsilon > 0$, the system is within the extended phase. For $\epsilon < 0$, $b$ and $b^2/c$ goes to infinity and consequently a transition to localization is expected. However we note that in this limit the perturbative expansion breaks down since $b, c$ increase under the RG flow. For $\epsilon = 0$, $b$ remains constant, $c$ goes slowly ($\sim 1/\log l$) to zero, and $b^2/c$ goes to infinity. That means that at the origin and for exponentially large volumes the eigenstates should be delocalized and the DoS is expected to diverge. Of course this divergence is somewhere cut off before the origin since random matrix theory (which should be valid in the deep infrared limit) predicts a vanishing of the DoS at the origin.

Finally we remark that the above pseudo-divergence is beyond the current numerical capabilities since $b \ll c$ and $1/c \sim \log l \sim \log n$ for $n \gg 1$.

## III. LEVEL CORRELATION FUNCTIONS

In this section we compute the DoS and the TLCF close to the origin in the $g \gg 1$ limit by using the nonlinear $\sigma$ model introduced in the previous section. As mentioned previously, in systems with chiral symmetry there is a clear distinction between the spectral correlations near zero (the origin) and away from zero (the bulk). In the bulk the spectral correlations are not affected by the block structure and coincide with the nonchiral version of Eq.(1) which has been intensively studied in recent years [23, 31]. After reviewing the result in the bulk, we examine the origin for the anomalous diffusion case $1/2 < \alpha \leq 3/2$. For normal diffusion, we refer to Ref.[32]. The case $\alpha = 1$, related to the Anderson transition, is worked out in detail.

### A. Review of results at the bulk

The use of the supersymmetry method permits an analytical evaluation of both spectral properties and eigenfunction statistics [23] in a certain region of parameters. In the thermodynamic limit it was found that the eigenfunctions are multifractal for $\alpha = 1$ and localized (delocalized) for $\alpha > 1$ ($\alpha < 1$) [23]. The spectral correlations in the limit $g = \pi E_c/\Delta \gg 1$ ($E_c$ the Thouless energy) can be expressed through the spectral determinant of a classical diffusion operator [15]. For the unitary ensemble

$$R(z) = 1 - \frac{1}{2z^2} - \frac{1}{4}\frac{\partial^2}{\partial z^2}\ln \mathcal{D}^2(z) + \frac{\cos(2z)}{2z^2}\mathcal{D}^2(z), \tag{22}$$

$$\mathcal{D}(z) = \prod_{n=1}^{\infty} \frac{g^2(2\pi n)^{2(2\alpha-1)}}{g^2(2\pi n)^{2(2\alpha-1)} + z^2}, \tag{23}$$

where $R(z) = \Delta^2\langle\rho(\epsilon_1)\rho(\epsilon_2)\rangle - 1$ is the TLCF, $\rho(\epsilon)$ is the DoS at energy $\epsilon$, $\Delta$ is the mean level spacing, $1/2 < \alpha \leq 3/2$, and the energy $z$ is expressed in units of $\Delta$ as $z = \pi(\epsilon_1 - \epsilon_2)/\Delta$. Although this result was derived assuming $z \gg 1$, in Ref.[33] it was shown that it is valid for all $z$.

We mention that the spectral determinant above corresponds with a process of anomalous diffusion [30] with $\langle|r|\rangle \propto t^{1/(2\alpha-1)}$. The asymptotic behavior of $R(z) \sim z^{-2+1/(2\alpha-1)}$ ($\alpha \neq 1$) is power-law and the dimensionless conductance $g \sim n^{2-2\alpha}$ increases (decreases) with the system size $n$ for $\alpha < 1$ ($\alpha > 1$). Both the scaling of $g$ and the TLCF resemble those of a weakly disordered conductor in $d = 2/(2\alpha - 1)$ dimensions [23]. For the special case $\alpha = 1$, $\mathcal{D}(z) = (z/2g)\sinh^{-1}(z/2g)$ and $R(z)$ can be explicitly evaluated as

$$R(z) = 1 - \frac{\sin^2 z}{z^2}\left(\frac{z/2g}{\sinh(z/2g)}\right)^2. \tag{24}$$

This correlation function reproduces typical features of the spectral correlations at the Anderson transition as level repulsion for $z \ll 1$ but sub-Poisson number variance $\Sigma^2(L) \sim \chi L$ for $L \gg 1$ (see Sec.IV for a definition of the number variance).

Although the RBM is defined in 1D, generalizations to $d$ dimensions are straightforward. In that case the product over $n$ runs over all possible $\vec{n} = (n_1, \ldots, n_d)$. As mentioned previously, according to Levitov's results [24], the properties of these power-law hopping models are similar in different dimensions provided that the dimension of the space is equal to the power-law decay. It is tempting to guess that a power-law decay $\alpha$ in $d = 1$ is similar to a decay $d\alpha$ in $d$ dimensions.

### B. Results at the origin

After reviewing the properties at the bulk we move to the spectral correlations close to the origin. In the limit $g = \pi E_c/\Delta = n^{2-2\alpha}/b \sim r_0^{2\alpha-1}n^{2-2\alpha} \gg 1$, we calculate the DoS and the TLCF of the chRBM (3) by using the nonlinear $\sigma$ model as given by Eq.(16) without the double trace term. As mentioned previously, since $b/c \sim 1/r_0 \ll 1$, the double-trace term can be safely neglected.

The DoS is given by the expression

$$\langle\rho(\epsilon)\rangle = \frac{1}{4\Delta V}\mathrm{Re}\int \mathcal{D}Q\left[\int dx \mathrm{str}\, k\Sigma_z Q(x)\right]\mathrm{e}^{-F}, \tag{25}$$

where $F$ is defined in Eq.(16). The perturbative calculation corresponds to expand the $Q$-matrix as

$$Q(x) = \Sigma_z \frac{1+iP}{1-iP} = \Sigma_z \left(1 + 2iP - 2P^2 + \cdots\right), \quad P = \begin{pmatrix} 0 & t \\ t & 0 \end{pmatrix}, \quad t = \begin{pmatrix} a & \sigma \\ \rho & ib \end{pmatrix}, \tag{26}$$

where $a$,$b$ are real variables and $\sigma$,$\rho$ Grassmann variables. The resulting expansion is in powers of the (anomalous) diffusion propagator

$$\Pi(q,\epsilon) = \frac{\Delta}{2\pi} \frac{1}{D|q|^{2\alpha-1} - i\epsilon}, \tag{27}$$

where $D = \Delta n/\pi b$. Finite $g$ corrections to the DoS are given by

$$\langle \rho(\epsilon) \rangle \sim \frac{1}{\Delta} \left[ 1 + \frac{1}{2} \mathrm{Re} \Big( \sum_q \Pi(q,\epsilon) \Big)^2 \right]. \tag{28}$$

Since the expansion is not well-defined for the zero mode ($q = 0$), this contribution should be removed from the above expression and treated in a separate way [34]. We remark, as was noticed in Ref.[32], the mean level spacing $\Delta$ corresponding to the ergodic regime is modified by a finite $g$ as

$$\frac{1}{\tilde{\Delta}} = \frac{1}{\Delta} \mathrm{Re} \int \mathcal{D}\tilde{Q} \left[ \frac{1}{4V} \int dx \mathrm{str}\, k\Sigma_z \tilde{Q}(x) \right] \mathrm{e}^{-F[\tilde{Q}]} \sim \frac{1}{\Delta} \left[ 1 + \frac{1}{2} \mathrm{Re} \Big( \sum_{q \neq 0} \Pi(q,\epsilon) \Big)^2 \right], \tag{29}$$

where $\tilde{Q}$ denotes the nonzero modes. This quantity is relevant for us since we are interested in level correlations of unfolded variables. Thus we define the DoS scaled in terms of the renormalized mean level spacing

$$\rho_1(z) = \tilde{\Delta} \langle \rho(\epsilon = \tilde{\Delta} z/\pi) \rangle. \tag{30}$$

We note that, as shown in Sec.IV, the renormalization of $\Delta$ is important to find agreement between the results of this section and those of Ref.[35].

The zero mode contribution is treated nonperturbatively and gives the ergodic result $g \to \infty$ [36]

$$\rho_1(z) \to \rho_1^{(0)}(z) = \frac{\pi z}{2} (J_0^2(z) + J_1^2(z)). \tag{31}$$

As in the nonchiral case [16], a proper parametrization of the $Q$-matrix is required to derive this expression. It can be incorporated into our $Q$-matrix as

$$Q(x) = T\tilde{Q}(x)\bar{T}, \tag{32}$$

where the supermatrix $T$ ($\bar{T}$ is the inverse of $T$) parametrizes the zero mode as [37]

$$\begin{aligned} T &= U T_0 \bar{U}, \\ T_0 &= \begin{pmatrix} \cos\frac{\hat{\theta}}{2} & -i\sin\frac{\hat{\theta}}{2} \\ -i\sin\frac{\hat{\theta}}{2} & \cos\frac{\hat{\theta}}{2} \end{pmatrix}, \quad \hat{\theta} = \begin{pmatrix} \theta_F & 0 \\ 0 & i\theta_B \end{pmatrix}, \\ U &= \begin{pmatrix} u & 0 \\ 0 & u \end{pmatrix}, \quad u = \exp \begin{pmatrix} 0 & \xi \\ \eta & 0 \end{pmatrix}, \end{aligned} \tag{33}$$

where $-\pi \leq \theta_F \leq \pi$, $0 \leq \theta_B \leq \infty$, and $\xi$ and $\eta$ are Grassmann variables. Using this parametrization, we integrate the zero mode first and, then, treat the nonzero modes perturbatively. This was done in Ref.[32] for the case of normal diffusion. In the present case, the zero mode part is unchanged since the kinetic term, second (and third) term in the free energy (16), does not include the zero mode. For the nonzero mode, the anomalous diffusion propagator Eq.(27) is used for the perturbative expansion. Thus after integration of the zero mode, we are left with,

$$\begin{aligned} \langle \rho(\epsilon) \rangle &\sim \frac{1}{\tilde{\Delta}} + \frac{\pi}{2\Delta} \mathrm{Re} \frac{d}{dz_0} \int_{z_0}^{\infty} dt (t - z_0) \left\langle J_0(t + z_0 A_B) J_0(t - z_0 A_F) - J_1(t + z_0 A_B) J_1(t - z_0 A_F) \right\rangle_{\mathrm{kin}}, \\ A_{F,B} &= -\frac{1}{2V} \int dx \mathrm{str}\, \frac{1 \pm k}{2} \Sigma_z [\tilde{Q}(x) - \Sigma_z], \\ \langle \cdots \rangle_{\mathrm{kin}} &= \int \mathcal{D}\tilde{Q} \, (\cdots) \exp \left[ -\frac{1}{4b} \int \frac{dq}{2\pi} |q|^{2\alpha-1} \mathrm{str}\, \tilde{Q}(q) \tilde{Q}(-q) \right], \end{aligned} \tag{34}$$

where $z_0 = \pi\epsilon/\Delta$ and $1/\tilde{\Delta}$ is the purely perturbative contribution (29). We note that this expression is valid up to second order in $1/g$. The ergodic result (31) can be easily recovered by putting $A_{F,B} = 0$.

We are now ready to evaluate Eq.(34) in different domains. In all cases the limit $g \gg 1$ is assumed. For $z \ll g$, known as the Kravtsov-Mirlin (KM) domain [34], the Bessel functions can be expanded in powers of $zA \sim z/g$ as

$$J(t - zA) \sim \left(1 - zA\frac{d}{dt} + \frac{z^2A^2}{2}\frac{d^2}{dt^2}\right) J(t), \tag{35}$$

to obtain

$$\langle\rho(\epsilon)\rangle \;\sim\; \frac{1}{\Delta}\mathrm{Re}\left[1 + \frac{1}{2}\langle A_B - A_F\rangle_{\rm kin}\frac{d}{dz_0}z_0 + \frac{1}{8}\left\langle(A_B - A_F)^2\right\rangle_{\rm kin}\frac{d}{dz_0}z_0^2\frac{d}{dz_0}\right]\rho_1^{(0)}(z_0). \tag{36}$$

Changing the variable from $z_0 = \pi\epsilon/\Delta$ to $z = \pi\epsilon/\tilde{\Delta}$, we finally are left with

$$\rho_1(z) \sim \left[1 + \frac{a_\alpha}{8g^2}\left(2z\frac{d}{dz} + z^2\frac{d^2}{dz^2}\right)\right]\rho_1^{(0)}(z), \tag{37}$$

where $\rho_1^{(0)}(z)$ is defined in Eq.(31) and $a_\alpha$ is the momentum summation for periodic boundary conditions,

$$a_\alpha = g^2\sum_{q\neq 0}\Pi^2(q,0) = 2\sum_{n=1}^{\infty}\frac{1}{(2\pi n)^{4\alpha-2}}. \tag{38}$$

We now move to the Andreev-Altshuler (AA) domain [15] $z \gg 1$. In this limit we cannot expand the Bessel functions. Instead we use their asymptotic form,

$$J_0(z) = \frac{1}{\pi}\int_0^\pi dx\mathrm{e}^{iz\cos x} \sim \sqrt{\frac{1}{\pi z}}\left[\left(1 - \frac{1}{8z} + \cdots\right)\cos z + \left(1 + \frac{1}{8z} + \cdots\right)\sin z\right]. \tag{39}$$

Noting that $J_1(z) = -J_0'(z)$ we find

$$\rho_1(z) \;\sim\; \mathrm{Re}\left[1 + \frac{1}{8z^2} - \frac{1}{2z}\mathrm{e}^{2iz}\int\mathcal{D}\tilde{Q}\mathrm{e}^{-F_k(z)}\right], \tag{40}$$

$$F_k(z) \;=\; \frac{1}{4b}\int\frac{dq}{2\pi}|q|^{2\alpha-1}\mathrm{str}\,\tilde{Q}(q)\tilde{Q}(-q) - \frac{iz}{2V}\int dx\mathrm{str}\,k\Sigma_z(\tilde{Q} - \Sigma_z). \tag{41}$$

We remark that the presence of the supermatrix $k = \mathrm{diag}(1,-1)$ breaks the supersymmetry in $F_k(z)$. Keeping terms up to second order in the $P$-matrix we obtain

$$\rho_1(z) \sim 1 - \frac{\cos 2z}{2z}\mathcal{D}(z) + \frac{1}{8z^2}, \tag{42}$$

where the spectral determinant $\mathcal{D}(z)$ is given by Eq.(23). We note that the ergodic limit corresponds to put $\mathcal{D} = 1$ which corresponds with the asymptotic form of the exact result Eq.(31).

We now consider the TLCF. In this case the analytical calculation is along the lines of the DoS though more technically involved. Here we present a summary of results. For technical details we refer to Ref.[32] where the case of normal diffusion was discussed. We start by defining

$$\rho_2(z_1,z_2) = \tilde{\Delta}^2\langle\langle\rho(\epsilon_1 = \tilde{\Delta}z_1/\pi)\rho(\epsilon_2 = \tilde{\Delta}z_2/\pi)\rangle\rangle, \tag{43}$$

where $\langle\langle\rho(\epsilon_1)\rho(\epsilon_2)\rangle\rangle = \langle\rho(\epsilon_1)\rho(\epsilon_2)\rangle - \langle\rho(\epsilon_1)\rangle\langle\rho(\epsilon_2)\rangle$ is the connected part of the TLCF. In the KM's domain $z_{1,2} \ll g$,

$$\rho_2(z_1,z_2) \;\sim\; -\left\{\left[1 + \frac{a_\alpha}{4g^2}\left(z_1\frac{\partial}{\partial z_1} + z_2\frac{\partial}{\partial z_2}\right) + \frac{a_\alpha}{8g^2}\left(z_1^2\frac{\partial^2}{\partial z_1^2} + 2z_1z_2\frac{\partial}{\partial z_1}\frac{\partial}{\partial z_2} + z_2^2\frac{\partial^2}{\partial z_2^2}\right)\right]K(z_1,z_2)\right\}^2, \tag{44}$$

where

$$K(z_1,z_2) = \frac{\pi\sqrt{z_1z_2}}{z_1^2 - z_2^2}(z_1J_1(z_1)J_0(z_2) - z_2J_0(z_1)J_1(z_2)). \tag{45}$$

The ergodic limit is given by $\rho_2(z_1,z_2)=-K^2(z_1,z_2)$. In the AA's domain $z_{1,2}\gg 1$,

$$\begin{aligned}\rho_2(z_1,z_2) \;\sim\; & \frac{1}{2}\mathrm{Re}\sum_{q^2\neq 0}\left(\Pi_+^2+\Pi_-^2\right)+\frac{\sin 2z_1}{2z_1}\mathcal{D}_1\mathrm{Im}\sum_{q^2\neq 0}\left(\Pi_++\Pi_-\right)+\frac{\sin 2z_2}{2z_2}\mathcal{D}_2\mathrm{Im}\sum_{q^2\neq 0}\left(\Pi_+-\Pi_-\right)\\ & +\frac{1}{8z_1z_2}\left[\mathcal{D}_1\mathcal{D}_2(\mathcal{D}_+^2\mathcal{D}_-^{-2}-1)\cos 2(z_1+z_2)+\mathcal{D}_1\mathcal{D}_2(\mathcal{D}_-^2\mathcal{D}_+^{-2}-1)\cos 2(z_1-z_2)\right]\\ & -\frac{1}{2(z_1+z_2)^2}\left[1+\mathcal{D}_1\mathcal{D}_2\mathcal{D}_+^2\mathcal{D}_-^{-2}\cos 2(z_1+z_2)\right]-\frac{1}{2(z_1-z_2)^2}\left[1-\mathcal{D}_1\mathcal{D}_2\mathcal{D}_-^2\mathcal{D}_+^{-2}\cos 2(z_1-z_2)\right]\\ & +\frac{1}{z_1^2-z_2^2}\left(\mathcal{D}_1\sin 2z_1-\mathcal{D}_2\sin 2z_2\right),\end{aligned} \tag{46}$$

where $\mathcal{D}_{1,2}=\mathcal{D}(z_{1,2})$, $\mathcal{D}_\pm=\mathcal{D}((z_1\pm z_2)/2)$, Eq.(23), and $\Pi_{1,2}=\Pi(q,\epsilon_{1,2})$, $\Pi_\pm=\Pi(q,(\epsilon_1\pm\epsilon_2)/2)$, Eq.(27). We remark that the first term of the r.h.s. is obtained by a purely perturbative calculation.

We stress that in the the common domain $1\ll z\ll g$ the results in both regions AA and KM coincide. It is worthwhile to note that in the unitary limit $z,z_1+z_2\to\infty$ our results also coincide with those of the nonchiral version of our model: $\rho_1(z)\to 1$ and

$$R(z_1,z_2)=1+\frac{\rho_2(z_1,z_2)}{\rho_1(z_1)\rho_1(z_2)}\to 1+\frac{1}{2}\mathrm{Re}\sum_{q^2\neq 0}\Pi_-^2-\frac{1}{2(z_1-z_2)^2}+\frac{\cos 2(z_1-z_2)}{2(z_1-z_2)^2}\mathcal{D}_-^2. \tag{47}$$

Noting $\Pi(q,\epsilon/2;g)=2\Pi(q,\epsilon;2g)$ and $\mathcal{D}(z/2;g)=\mathcal{D}(z;2g)$, we see that this is the AA's result (22) for the unitary class where $g$ is substituted by $2g$. The factor 2 is considered to be due to the chiral symmetry.

### C. Explicit results for $\alpha=1$

The case $\alpha=1$ is specially interesting. On the one hand it is related to the spectral correlations at the Anderson transition and on the other hand the analytical results of the previous section are greatly simplified since the spectral determinant can be evaluated exactly.

In the KM domain the summation in $a_\alpha$ can be easily performed,

$$a_1=\frac{1}{2\pi^2}\sum_{n=1}^{\infty}\frac{1}{n^2}=\frac{1}{12}. \tag{48}$$

The DoS and the TLCF are consequently given by

$$\rho_1(z) \;\sim\; \left[1+\frac{1}{96g^2}\left(2z\frac{d}{dz}+z^2\frac{d^2}{dz^2}\right)\right]\rho_1^{(0)}(z), \tag{49}$$

$$\rho_2(z_1,z_2) \;\sim\; -\left\{\left[1+\frac{1}{48g^2}\left(z_1\frac{\partial}{\partial z_1}+z_2\frac{\partial}{\partial z_2}\right)+\frac{1}{96g^2}\left(z_1^2\frac{\partial^2}{\partial z_1^2}+2z_1z_2\frac{\partial}{\partial z_1}\frac{\partial}{\partial z_2}+z_2^2\frac{\partial^2}{\partial z_2^2}\right)\right]K(z_1,z_2)\right\}^2. \tag{50}$$

The results in AA's domain $1\ll z_{1,2}$, $1\ll g$ are greatly simplified since both the spectral determinant

$$\mathcal{D}(z)=\prod_{n=1}^{\infty}\frac{1}{1+(z/2\pi gn)^2}=\frac{z/2g}{\sinh(z/2g)}, \tag{51}$$

and the momentum summations of the propagator can be exactly evaluated,

$$\begin{aligned}\mathrm{Re}\sum_{q^2\neq 0}\Pi^2(q,\epsilon)&=\frac{1}{8\pi^2g^2}\mathrm{Re}\sum_{n=1}^{\infty}\frac{1}{(n-iz/2\pi g)^2}=\frac{1}{4z^2}\left(1-\mathcal{D}^2(z)\right),\\ \mathrm{Im}\sum_{q^2\neq 0}\Pi(q,\epsilon)&=\frac{i}{4\pi g}\sum_{n=1}^{\infty}\left(\frac{1}{n+iz/2\pi g}-\frac{1}{n-iz/2\pi g}\right)=-\frac{1}{2z}\left(1-\frac{z}{2g}\coth\frac{z}{2g}\right).\end{aligned} \tag{52}$$

By utilizing the relations

$$\begin{aligned}\frac{1}{2g}\left(\coth\frac{z_1+z_2}{4g}+\coth\frac{z_1-z_2}{4g}\right) &= \frac{4z_1}{z_1^2-z_2^2}\mathcal{D}_1^{-1}\mathcal{D}_+\mathcal{D}_-,\\ \mathcal{D}_1\mathcal{D}_2(\mathcal{D}_+^2\mathcal{D}_-^{-2}-1) &= -\frac{4z_1z_2}{(z_1-z_2)^2}(\mathcal{D}_+^2-\mathcal{D}_1\mathcal{D}_2),\end{aligned} \tag{53}$$

we find the following simple form for the TLCF,

$$\rho_2(z_1,z_2) = -\left[\frac{\sin(z_1-z_2)}{z_1-z_2}\mathcal{D}_- - \frac{\cos(z_1+z_2)}{z_1+z_2}\mathcal{D}_+\right]^2. \tag{54}$$

We easily see that the unitary limit $z_1+z_2\to\infty$, Eq.(24), can be recovered by keeping only the first term in the bracket.

## IV. CHIRAL SYMMETRY AND ANDERSON TRANSITION

In this section, for the special value $\alpha=1$, we put forward an exact result for the DoS and the TLCF, valid for all $z, z_{1,2}$, in the limit $g\gg 1$. The spectral fluctuations in this case present features as scale invariance, level repulsion, and asymptotically linear number variance similar to the ones at the Anderson transition. Thus the chRBM at $\alpha=1$ is an ideal candidate to investigate the interplay between chiral symmetry and wavefunction localization leading to the Anderson transition. We recall that in the thermodynamic limit, according to the RG analysis of previous sections, the chiral symmetry will delocalize the eigenstates close to the origin and the DoS is divergent (though according to chiral random matrix prediction this divergence is cut off before the origin).

### A. Generalized chiral random matrix model for critical statistics

We find exact expressions for the DoS and TLCF of the chRBM at $\alpha=1$ by mapping it onto an exactly solvable generalized chiral random matrix model (gchRMM). The model in question is defined by the probability density

$$P(\mathcal{H}) \propto \int \mathcal{D}U \exp \mathrm{Tr}\left[-\frac{1}{4h}\mathcal{H}^2 - n^2 h[\mathcal{H},U][\mathcal{H},U]^\dagger\right], \tag{55}$$

where $\mathcal{H}$ is given by Eq.(1), $U$ has the chiral block structure

$$U = \begin{pmatrix} U_1 & 0 \\ 0 & U_2 \end{pmatrix}, \tag{56}$$

with $U_{1,2}$ $n\times n$ unitary matrices, and $\mathcal{D}U$ denotes the Haar measure of the unitary matrices $U_{1,2}$. We shall see that the parameter $h$ is indeed related to the conductance $g$ by $h\sim 1/g$. In Refs.[38, 39], it was found that the spectral correlations of this model are equivalent to the spatial correlations of the Calogero-Sutherland (CS) model [40] at finite temperature. By using this analogy, exact expressions for the spectral correlations were found for any $g\sim 1/h$. It turns out that in the $g\gg 1$ limit such model is also equivalent to our chRBM at $\alpha=1$ [41]. The argument is as follows. By decomposing Eq.(55) into the blocks of $\mathcal{H}$ and $U$, the probability density can be written as

$$P(\mathcal{H}) \propto \int \mathcal{D}U \exp \mathrm{Tr}\left[-\frac{1+8h^2n^2}{2h}CC^\dagger + 4n^2 h \mathrm{Re} U_1 C U_2 C^\dagger\right]. \tag{57}$$

The integral over $U$ is, in principle, performed by using the Harish-Chandra-Itzykson-Zuber formula. However one could attempt an alternate route. Random matrix theory predicts that the spectral density of $U$ in the large $n$ limit is constant and, due to level repulsion, the eigenvalues are consequently well separated. One can thus model the spectrum typical of a $U$ as $\exp(i\theta_m)$ $(m=1,\dots 2n)$ where in a first approximation the phases $\theta_m = 2\pi m/2n$ are assumed to be equidistant. By doing that we are neglecting the small fluctuations around the equidistant position. Within these approximations the integral over $U$ is reduced, up to multiplicative constant factors, to the contribution of one "typical" $U$. In a basis such that the $U_{1,2}$ in (57) becomes diagonal,

$$P(\mathcal{H}) \propto \exp\left\{\sum_{i,j}|C_{ij}|^2\left[1+(4nh)^2\sin^2\frac{\pi(i-j)}{2n}\right]\right\}. \tag{58}$$

This expression describes a chRBM with variance

$$a^2(r=|i-j|) \sim \frac{1}{1+(4nh)^2\sin^2\frac{\pi r}{2n}} \sim \frac{1}{1+4\pi^2h^2r^2}, \tag{59}$$

but this is nothing but our original chRBM for $\alpha = 1$ with $r_0 \sim 1/h$. Thus the spectral correlations of both models should coincide. Let us first review the exact results for the gchRMM reported in Ref.[35]. In the $h \ll 1$ limit, the DoS was found to be

$$\langle \rho(\epsilon) \rangle = \frac{1}{\Delta} \int_{-1/h}^{\infty} dt \frac{(1+ht)^2}{\cosh^2\left[2t(1+\frac{ht}{2})\right]} \rho_1^{(0)}\left((1+ht)\frac{\pi\epsilon}{\Delta}\right), \tag{60}$$

where $\Delta = \pi/2n$ is the mean level spacing at $h = 0$, and $\rho_1^{(0)}(z)$ is given by Eq.(31). The TLCF is

$$\langle\langle \rho(\epsilon_1)\rho(\epsilon_2) \rangle\rangle = -\frac{1}{\Delta^2}\left[\int_{-1/h}^{\infty} dt \frac{(1+ht)^2}{\cosh^2\left[2t(1+\frac{ht}{2})\right]} K\left((1+ht)\frac{\pi\epsilon_1}{\Delta}, (1+ht)\frac{\pi\epsilon_2}{\Delta}\right)\right]^2, \tag{61}$$

where $K(z_1, z_2)$ is given by Eq.(45).

The mean level spacing $\Delta(h)$ at $h \neq 0$ can be evaluated from Eq.(60) as

$$\frac{1}{\Delta(h)} = \frac{1}{\Delta} \int_{-1/h}^{\infty} dt \frac{(1+ht)^2}{\cosh^2\left[2t(1+\frac{ht}{2})\right]} \sim \frac{1}{\Delta}\left(1 - \frac{\pi^2 h^2}{96}\right). \tag{62}$$

We note that this quantity corresponds to $\tilde{\Delta}$ in Eq.(29). Naive calculation of $\tilde{\Delta}$ using the nonlinear $\sigma$ model gives a divergent result and we thus find disagreement with Eq.(62). However, just like in Eqs.(30) and (43), if the above results are scaled in terms of $\Delta(h)$ as

$$\begin{aligned} \rho_1(z) &= \Delta(h)\langle \rho(\epsilon = \Delta(h)z/\pi) \rangle, \\ \rho_2(z_1, z_2) &= \Delta^2(h)\langle\langle \rho(\epsilon_1 = \Delta(h)z_1/\pi)\rho(\epsilon_2 = \Delta(h)z_2/\pi) \rangle\rangle, \end{aligned} \tag{63}$$

we show below that agreement between both calculations is found.

In order to prove this claim we perform a series expansion on the exact results (60) and (61) to compare them with the findings of the previous section in both the AA and KM domain. For the KM domain we start with the expression (60). The integral is strongly peeked around $t = 0$. Therefore we can perform an expansion in powers of $t$ up to terms involving $h^2$ corrections.

$$\begin{aligned} \langle \rho(\epsilon) \rangle &\sim \frac{1}{\Delta} \int_{-1/h}^{\infty} dt \frac{1}{\cosh^2 2t} \left(1 + 2ht - 2ht^2 \frac{\sinh 2t}{\cosh 2t} + h^2t^2 - 4h^2t^3 \frac{\sinh 2t}{\cosh 2t} - h^2t^4 + 3h^2t^4 \frac{\sinh^2 2t}{\cosh^2 2t}\right) \\ &\quad \times \left(1 + htz\frac{d}{dz} + \frac{h^2t^2}{2} z^2 \frac{d^2}{dz^2} + \frac{\pi^2 h^2}{96} z \frac{d}{dz}\right) \rho_1^{(0)}(z) \\ &\sim \frac{1}{\Delta(h)} \left[1 + \frac{\pi^2 h^2}{96}\left(2z\frac{d}{dz} + z^2\frac{d^2}{dz^2}\right)\right] \rho_1^{(0)}(z). \end{aligned} \tag{64}$$

The TLCF is calculated in the same way. After a laborious calculation one is left with

$$\begin{aligned} \langle\langle \rho(\epsilon_1)\rho(\epsilon_2) \rangle\rangle &\sim -\frac{1}{\Delta^2(h)} \left\{ \left[1 + \frac{\pi^2 h^2}{48}\left(z_1\frac{d}{dz_1} + z_2\frac{d}{dz_2}\right)\right.\right. \\ &\quad \left.\left. + \frac{\pi^2 h^2}{96}\left(z_1^2\frac{d^2}{dz_1^2} + 2z_1z_2\frac{d}{dz_1}\frac{d}{dz_2} + z_2^2\frac{d^2}{dz_2^2}\right)\right] K(z_1, z_2)\right\}^2. \end{aligned} \tag{65}$$

In the AA's domain $1 \ll z, z_{1,2}$, the DoS reduces to

$$\begin{aligned} \langle \rho(\epsilon) \rangle &\sim \frac{1}{\Delta(h)} \int_{-\infty}^{\infty} dt \frac{1}{\cosh^2 2t} \left[1 - \frac{\cos\left[2z(1+ht)\right]}{2z} + \frac{1}{8z^2}\right] \\ &= \frac{1}{\Delta(h)} \left[1 - \frac{\cos 2z}{2z}\mathcal{D}(z) + \frac{1}{8z^2}\right], \end{aligned} \tag{66}$$

where

$$\mathcal{D}(z) = \int_{-\infty}^{\infty} dt \frac{\cos(2zht)}{\cosh^2(2t)} = \frac{\pi hz/2}{\sinh(\pi hz/2)}. \tag{67}$$

In a similar way, by using

$$K(z_1,z_2) \sim \frac{\sin(z_1-z_2)}{z_1-z_2} - \frac{\cos(z_1+z_2)}{z_1+z_2}, \tag{68}$$

we obtain for the TLCF

$$\langle\langle \rho(\epsilon_1)\rho(\epsilon_2)\rangle\rangle \;\sim\; -\frac{1}{\Delta^2(h)}\left[\frac{\sin(z_1-z_2)}{z_1-z_2}\mathcal{D}\left(\frac{z_1-z_2}{2}\right) - \frac{\cos(z_1+z_2)}{z_1+z_2}\mathcal{D}\left(\frac{z_1+z_2}{2}\right)\right]^2. \tag{69}$$

As expected these results are in complete agreement with the findings of the previous section by setting $h = 1/\pi g$. We note that the function $\mathcal{D}(z)$ in Eq.(23) can be written in a spectral determinant form

$$\mathcal{D}(z) = \prod_{n=1}^{\infty} \frac{n^2}{n^2 + h^2 z^2/4}. \tag{70}$$

We remark that the mapping proposed in this section provides with explicit exact results for any value of $z$. Concerning the relation with the spectral properties at the Anderson transition we mention that in Ref.[35] it was shown analytically that the gchRMM (and consequently our chRBM at $\alpha = 1$) reproduces all the features of critical statistics. We do not repeat here this discussion and refer to it for details and to the next section for numerical verification.

Once we have proposed exact relations for the spectral correlations at the special value $\alpha = 1$, it is worthwhile to ask whether an analogous result can be extended for the rest of $\alpha$s. Unfortunately a mapping as the one above reported for $\alpha = 1$ cannot be extended to other values of $\alpha$. We attempt a different strategy. The DoS (60) and the TLCF (61) were explicitly evaluated in Ref.[35] in the large conductance $g = 1/\pi h \gg 1$ limit. The resulting expressions, valid up to $1/g^2$ corrections, were derived keeping the combination $z/g$ fixed. This amounts to neglect $z^k/g^{k+2}$ terms as compared to $z^k/g^k$. We remark that this expansion coincides with the supersymmetry calculation in the AA domain but not in the KM domain where $1/g^2$ corrections were kept. The results of Ref.[35] (Eqs.(61) and (69) there) can be rewritten in the following way,

$$\rho_1(z) \;=\; \frac{\pi z}{2}(J_0^2(z)+J_1^2(z)) + \frac{\pi}{2}J_0(z)J_1(z)(\mathcal{D}(z)-1), \tag{71}$$

$$\begin{aligned}\rho_2(x,y) \;=\; & \frac{1}{2}\mathrm{Re}\sum_{q\neq 0}\left(\Pi_+^2+\Pi_-^2\right) + \frac{\mathcal{D}_+^2-1}{2(x+y)^2} + \frac{\mathcal{D}_-^2-1}{2(x-y)^2} \\ & -\left\{\frac{\pi\sqrt{xy}}{2(x+y)}\mathcal{D}_+\left[J_1(x)J_0(y)+J_0(x)J_1(y)\right] + \frac{\pi\sqrt{xy}}{2(x-y)}\mathcal{D}_-\left[J_1(x)J_0(y)-J_0(x)J_1(y)\right]\right\}^2,\end{aligned} \tag{72}$$

where $\mathcal{D}_\pm = \mathcal{D}((x\pm y)/2)$ and $\Pi_\pm^2 = \Pi^2(q,(x\pm y)/2)$ with $\mathcal{D}$ and $\Pi$ given by Eqs.(51) and (27) at $\alpha = 1$ respectively. These expressions are consistent with Eqs.(42) and (54). For $\alpha = 1$, using the relation (52), the first line of the r.h.s of Eq.(72) vanishes. The reason of keeping the expression of the first line is that we want to separate purely perturbative contributions involving the propagator $\Pi$ from the nonperturbative ones.

Since the dependence in $\alpha$ above is only through $\mathcal{D}$ and $\Pi$, we speculate that for general $\alpha$ the expressions for the DoS and the TLCF of our chRBM (in the $g \gg 1$ limit) are given by the above expressions with $\mathcal{D}$ and $\Pi$ replaced by Eqs.(23) and (27) respectively. For the DoS, this speculation is supported by the supersymmetric calculation (which is valid for arbitrary $\alpha$) since Eq.(71) is consistent with Eq.(42). For the TLCF the situation is less clear. The supersymmetry result for the TLCF at $\alpha \neq 1$ has a complicated form (46) due to the nontrivial mixing of perturbative and nonperturbative contributions. We remark that for the special value $\alpha = 1$ it was greatly simplified to Eq.(54) by using nontrivial relations of the propagator and the spectral determinant as demonstrated in Sec.III C. We could not manage to recast (46) as in Eq.(72). We thus conclude that Eq.(72) for arbitrary $\alpha$ is just the simplest alternative among several possible options.

### B. Numerical results

We now compare the analytical predictions of previous sections with the results of direct numerical diagonalization of the chRBM in the spectral region close to the origin. Since we are mainly interested in the spectral correlations beyond the Thouless energy attention is focused on long range correlators as the number variance $\Sigma^2(L) = \langle L\rangle^2 - \langle L^2\rangle = \int_0^{\pi L} dz\rho_1(z) - \int_0^{\pi L} dxdyR(x,y)$. We recall that the number variance $\Sigma^2(L)$ measures the stiffness of the spectrum. In the metallic regime, for eigenvalues separated less than the Thouless energy, fluctuations are small and

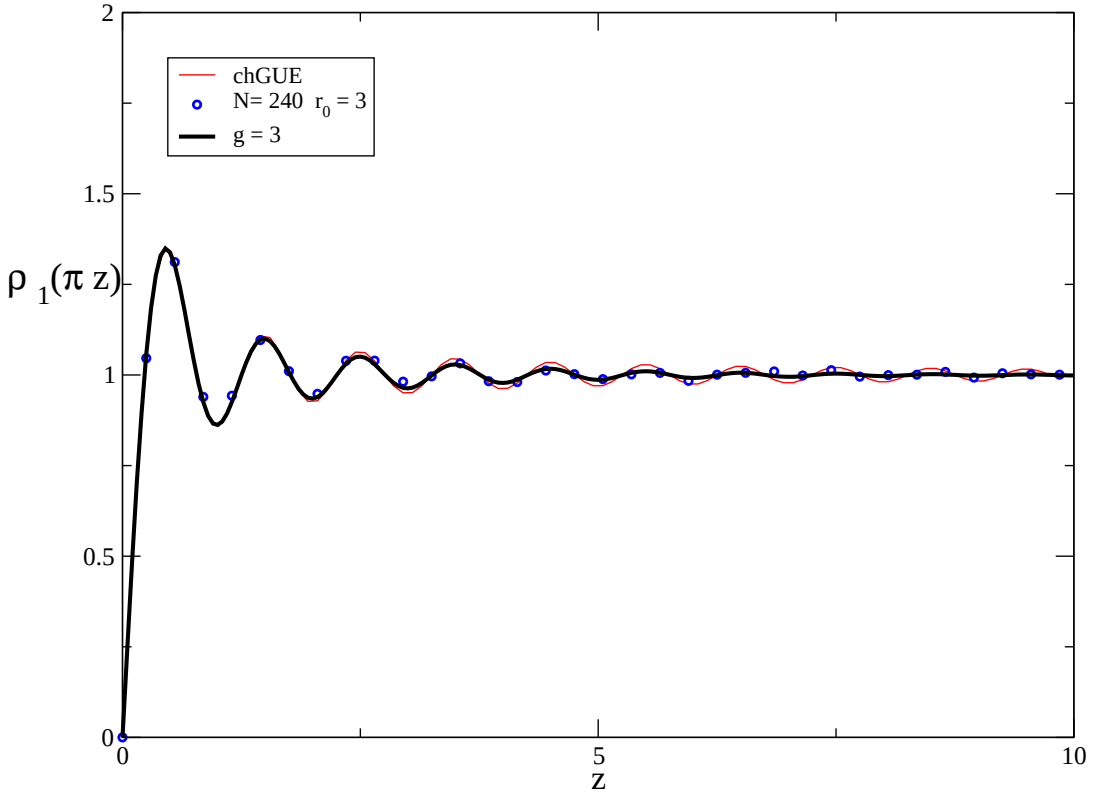


FIG. 1: DoS $\rho_1(z)$. The solid line is the analytical prediction of the chRBM (71) at a given $g$. The symbols represent the numerical results for the indicated volume $N$ and bandwidth $r_0$, and the thin line stands for the result at ergodic limit $g \to \infty$ (chiral Gaussian unitary ensemble (chGUE)). As observed the agreement with the analytical results is impressive.

$\Sigma^2(L) \sim \log(L)$ for $L \gg 1$. Beyond the Thouless energy spectral fluctuations get stronger and $\Sigma^2(L) \sim L^{d/2}$, where $d$ is the dimensionality of the space. For disorder strong enough eigenvalues are uncorrelated (Poisson statistics) and $\Sigma^2(L) = L$. At the Anderson transition, the number variance is asymptotically proportional to $\chi L$ ($\chi < 1$) [21]. The spectral fluctuations are studied by direct diagonalization of the chRBM for different sizes ranging from $N = 2n = 240$ to $N = 2n = 1200$. The eigenvalues thus obtained are unfolded with respect to the mean DoS. The number of different realizations of disorder is chosen such that for each $N$ the total number of eigenvalue be at least $2 \times 10^5$. In order to reduce unwanted finite size effects we have utilized a "periodic boundary" version of Eq.(1) as in Ref.[31].

We first study the spectral fluctuations at the critical value $\alpha = 1$. In this case, since the spectral determinant can be explicitly evaluated, both the DoS (71) and the TLCF (72) have a simple form. It is straightforward to show analytically [35] that $\Sigma^2(L) \sim L/4\pi r_0$ for $L \gg 1$. In Fig.1 we show the numerical DoS versus the analytical prediction (71). As observed, the oscillations of the DoS are damped with respect to the ergodic regime. We stress that, since $g = r_0$, the comparison between analytical and numerical is parameter free.

One of the signatures of an Anderson transition is the independence of $g$ on the system size. In our case, analytically it is also predicted that $g = r_0$ ($r_0 \gg 1$) is scale invariant. In Fig.2 the number variance for $r_0 = 3$ and $\alpha = 1$ is plotted for different volumes $N$. As expected the spectrum is scale invariant as at the Anderson transition. In Fig.3 we test our analytical findings by comparing them with the numerical number variance at the origin for different matrix sizes and bandwidth $r_0 = 3$. As observed, the theoretical predictions are fully confirmed. The deviations appearing after $L \sim 20$ are a well understood finite size effect.

We now study the spectral correlations for non critical values of $\alpha$. For $1/2 < \alpha < 1$, according to our conjecture Eq.(72), the asymptotic value of the TLCF is controlled by the power-law tail of the perturbative part. Thus it is expected that for $L \gg 1$, $\Sigma^2(L) \sim L^{1/2\alpha-1}$. The dimensionless conductance $g \sim r_0^{2\alpha-1} N^{2-2\alpha}$ increases as the system size does. In Fig.4 we show the numerical number variance for different $\alpha$s versus the conjecture Eq.(72). The numerical number variance follows the expected asymptotic power-law behavior in fair agreement with the conjectured result. This evidence is not conclusive since different conjectures with the same asymptotic limits also may be in good agreement with the numerical results. Clearly further work is needed to settle this issue.

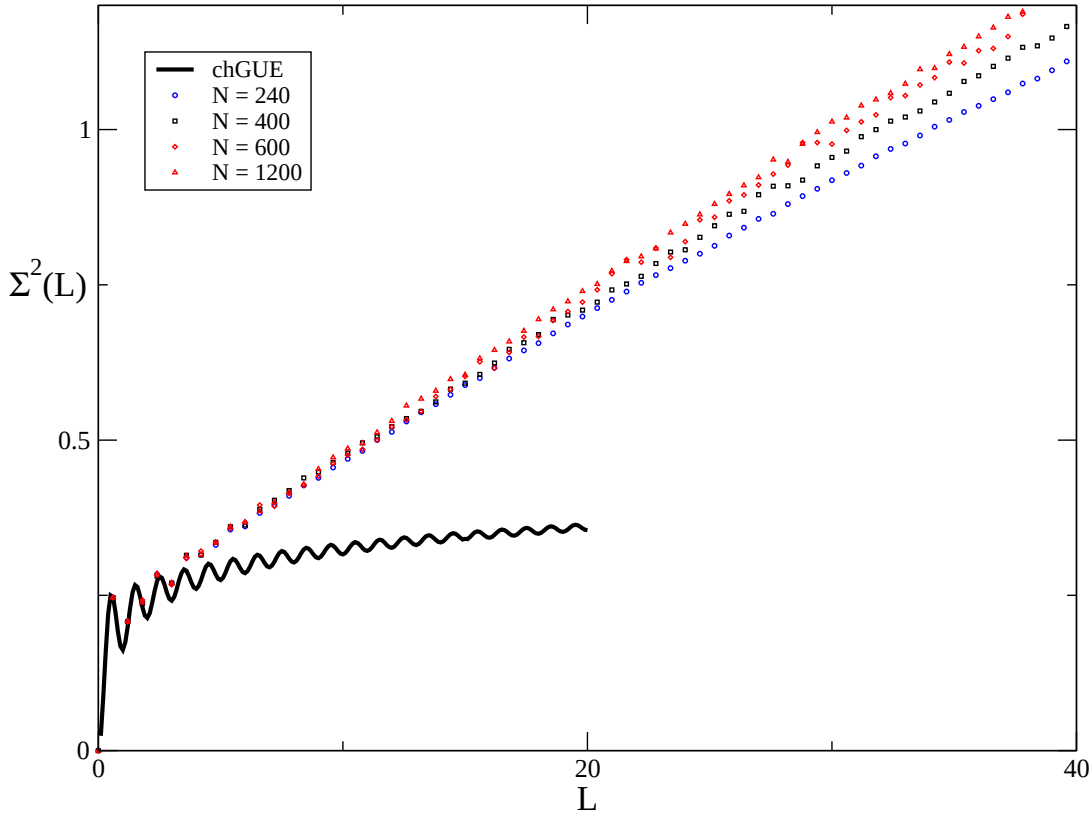


FIG. 2: Number variance $\Sigma^2(L)$ close to the origin of the spectrum. The symbols represent the numerical results for the indicated volume $N$ and bandwidth $r_0 = 2$. As observed, the spectrum is scale invariant. Differences for large distances are due to finite size effects.

## V. APPLICATIONS: THE QCD VACUUM AS A DISORDERED MEDIUM

In this section we discuss applications of our results in the context of QCD. Generally, for $\alpha > 3/2$ corresponding to normal diffusion, our model should describe the leading finite $g$ corrections to the spectral correlations of any disorder system with short range disorder and chiral symmetry. The case of $1/2 < \alpha \leq 3/2$ corresponds with chiral disordered systems with long range hopping. This is typical of systems driven by dipole interactions $(1/r^3)$ [24]. We would also like to mention that for $\alpha = 1$ our results provide a phenomenological description of the properties of systems with chiral symmetry at the Anderson transition. Before going into details a word of caution is in order. As mentioned in the introduction, the spectral correlations of chiral systems, unlike for the standard universality class, are highly dependent on microscopical details of the model as the exact form of the disordered potential. Thus the applications below reported must be considered as educated guesses among a broad class of systems in which our findings may be relevant.

In the infrared limit the eigenvalue correlations of the QCD Dirac operator do not depend on the dynamical details of the QCD Lagrangian but only on the global symmetries of the QCD partition function [2]. Thus random matrices with the correct chiral symmetry of QCD (termed chiral random matrices) [6] accurately describe the spectral properties of the QCD Dirac operator up to some scale known as the Thouless energy. For larger energy differences, dynamic features become important and the standard random matrix model ceases in principle to be applicable. However, in a recent work [42], it has been reported that the spectral correlations of the QCD Dirac operator in a background of instantons are accurately described by a chiral RBM with $\alpha = 3/4$ up to scales well beyond the Thouless energy. The reason for such exponent is indeed related to the dipole-like interaction dominating the interaction between quark zero modes and instantons. The matrix elements $T_{\rm IA}$ (which physically describe the amplitude of probability for a quark to hop from an instanton to an antiinstanton) of the QCD Dirac operator in a basis of chiral zero modes decay as $T_{\rm AI} \sim 1/R_{\rm IA}^3$ (dipole-like interaction) where $R_{\rm IA}$ is the instanton-antiinstanton distance in a 4D space. It was shown in Ref.[24] that the spectral properties of systems with power-law hopping are similar in different dimensions provided that the decay exponent matches the space dimension. Thus a decay $T_{\rm AI} \sim 1/R_{\rm IA}^3$ in 4D is equivalent to $T_{\rm AI} \sim 1/R_{\rm IA}^{3/4}$ in 1D. Furthermore, with this value of $\alpha$, $g$ scales at the bulk as a 4D conductor ($g \sim \sqrt{n}$) which is the expected result

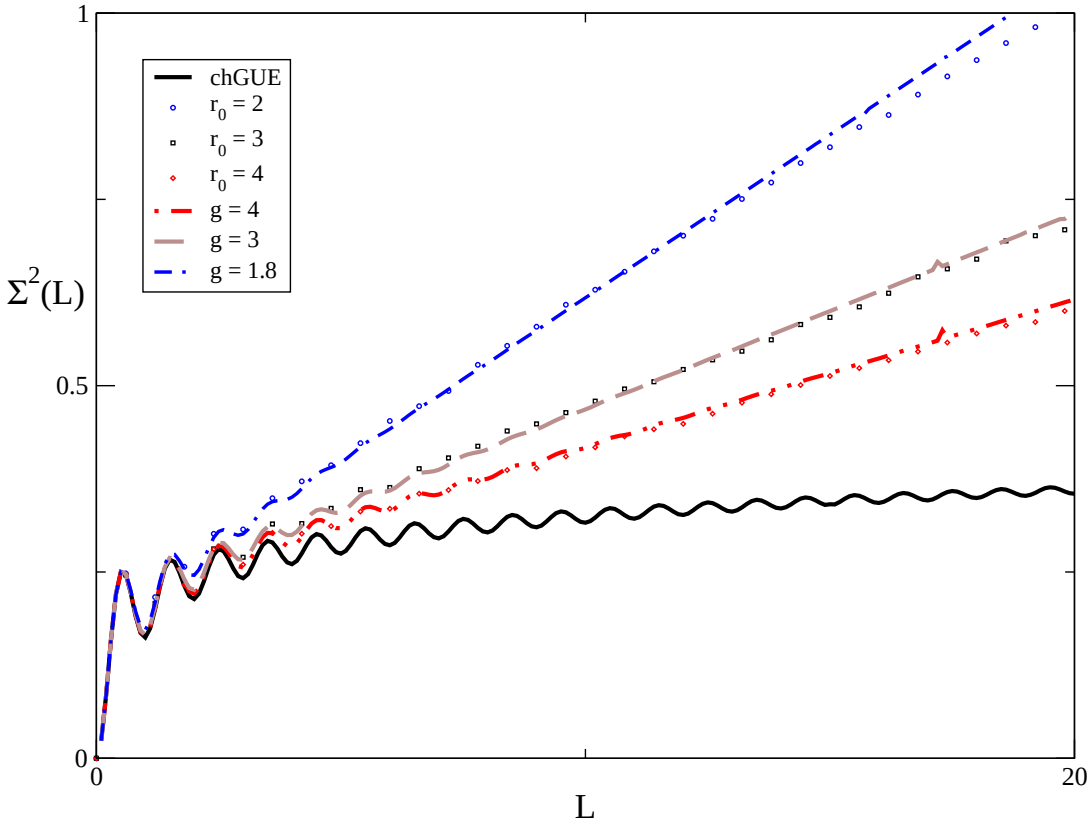


FIG. 3: Number variance $\Sigma^2(L)$ close to the origin of the spectrum for $\alpha = 1$. The solid lines are the analytical predictions for the chRBM Eqs.(71) and (72), and the symbols represent the numerical results for the indicated bandwidth $r_0$ and $N = 400$. As observed, the agreement with the analytical results is remarkable. The value of $g$ chosen corresponds with the analytical prediction except for $r_0 = 2$ where the best fitting is for $g = 1.8$ instead of $g = 2$. This deviation is expected since the analytical predictions are valid only in the $g \gg 1$ limit.

from chiral perturbation theory [43] and lattice simulations [44]. The range of applicability of this chRBM was found not to be restricted to the above mentioned zero temperature case. As usual in field theory, temperature is introduced by compactifying one of the spatial dimensions. Thus in Euclidean QCD the effect of temperature is to reduce the effective dimensionality of the system to three. Now since the effective dimension of the space matches the power-law decay of the QCD Dirac operator ($\sim 1/R^3$) one expects, according to Refs.[24, 45], multifractal wavefunctions typical of a metal-insulator transition. As mentioned previously, this situation corresponds with the case $\alpha = 1$ in our chRBM. The above findings suggest that, in case that the restoration of the chiral symmetry expected at finite temperature were dominated by instantons, the physical mechanism leading to the quark-gluon plasma state of matter could be similar to an Anderson transition driven by dipole interactions.

## VI. CONCLUSION

We have studied the spectral properties of a disordered system with chiral symmetry and long range hopping. By mapping the problem to a supersymmetric nonlinear $\sigma$ model we have obtained explicit expression for both the DoS and TLCF in different domains. It has been observed that, as in the nonchiral case, if the power-law decay matches the dimensionality of the space the spectral correlations are similar to the ones at the Anderson transition and are described by critical statistics. Based on the relation with a gchRMM we have put forward an exact formula for a specific value ($\alpha = 1$) of the power-law decay and we have also speculated that a similar relation should hold for the rest of $\alpha$s. Finally we have argued that in the context of QCD, our model may be utilized to describe the spectral correlations of the QCD Dirac operator beyond the Thouless energy at zero and at finite temperature.

A.M.G. was supported by the EU network “Mathematical aspects of quantum chaos”. K.T was supported by

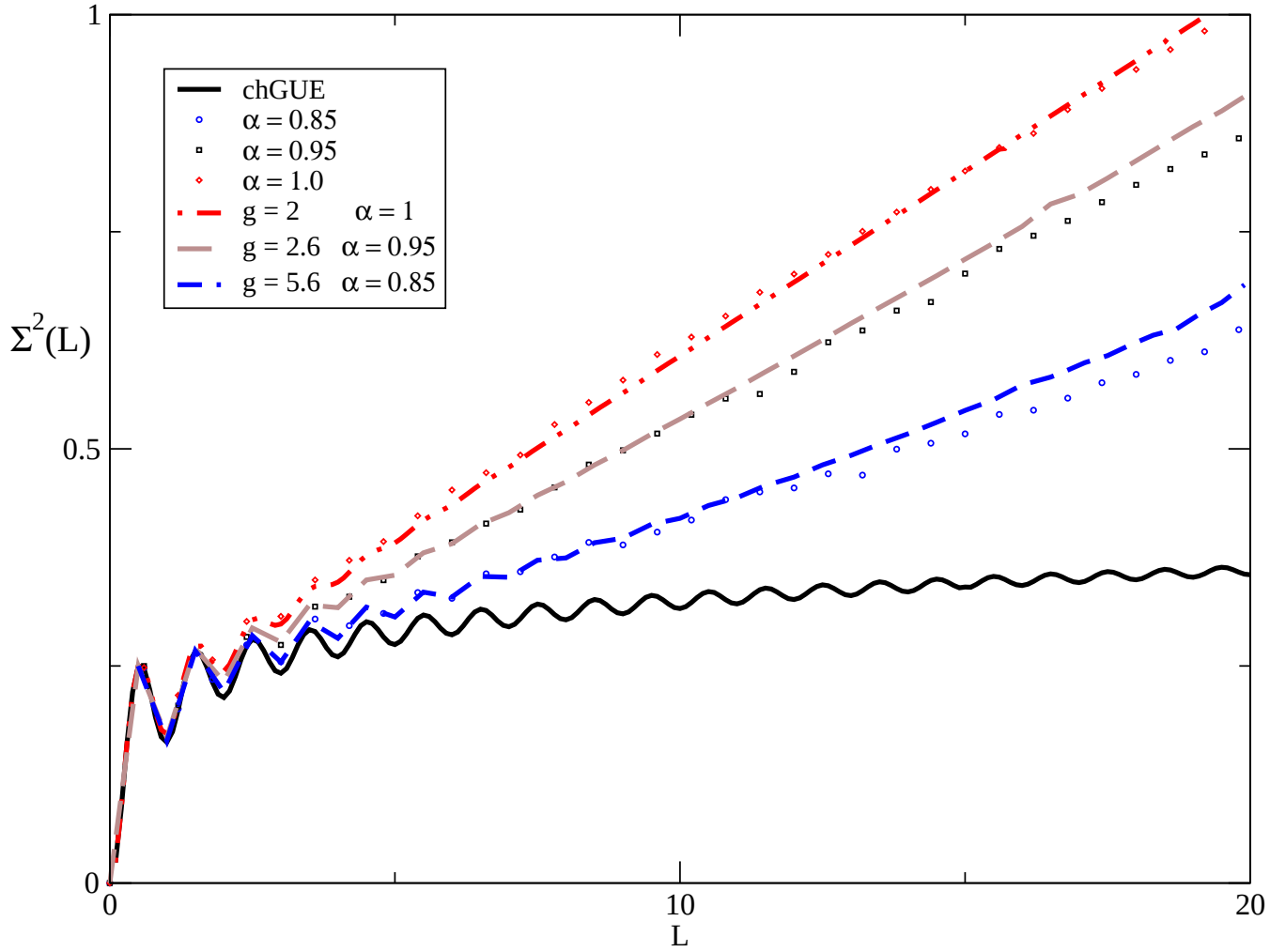


FIG. 4: Number variance $\Sigma^2(L)$ close to the origin of the spectrum in the delocalized regime $\alpha \leq 1$. The symbols correspond with the numerical simulation. The lines correspond with the analytical number variance with $R(x,y)$ given by the conjecture Eq.(72). In all cases $N$ in set to $N = 400$ and $r_0 = 2$. The value of $g$ chosen is the best fit to the numerical results. We checked that it is close ($\pm 5\%$) to the analytical prediction, $g \sim r_0^{2\alpha-1} N^{2-2\alpha}$ [23].

SFB/Transregio 12.

[1] E.P. Wigner, Ann. Math. **53**, 36 (1951); F.J. Dyson, J. Math. Phys. **3**, 140, 157, 166 (1962).
[2] E.V. Shuryak and J.J.M. Verbaarschot, Nucl. Phys. **A560**, 306 (1993).
[3] K. Slevin and T. Nagao, Phys. Rev. Lett. **70**, 635 (1993).
[4] M.R. Zirnbauer, J. Math. Phys. **37**, 4986 (1996).
[5] A. Altland and M.R. Zirnbauer, Phys. Rev. B **55**, 1142 (1997).
[6] J.J.M Verbaarschot, Phys. Rev. Lett. **72**, 2531 (1994).
[7] J.C. Osborn and J.J.M. Verbaarschot, Phys. Rev. Lett. **81**, 268 (1998); Nucl. Phys. **B525**, 738 (1998).
[8] A. Altland and B.D. Simons, Nucl. Phys. **B562**, 445 (1999).
[9] V. Gurarie and J.T. Chalker, Phys. Rev. Lett. **89**, 136801 (2002).
[10] A. Altland, Phys. Rev. B **65**, 104525 (2002); W.A. Atkinson, P.J. Hirschfeld, A.H. Macdonald, and K. Ziegler, Phys. Rev. Lett. **85**, 3926 (2000).
[11] A. Altland and R. Merkt, Nucl. Phys. **B607**, 511 (2001); P. Brouwer, C. Mudry, and A. Furusaki, Phys. Rev. Lett. **84**, 2913 (2000).
[12] R. Gade, Nucl. Phys. B **398**, 499 (1993).
[13] C. Pépin and P.A. Lee, Phys. Rev. Lett. **81**, 2779 (1998).

[14] A. Furusaki, Phys. Rev. Lett. **82**, 604 (1999).
[15] A.V. Andreev and B.L. Altshuler, Phys. Rev. Lett. **75**, 902 (1995); A.V. Andreev, B.D. Simons and B.L. Altshuler, J. Math. Phys. **37**, 4968 (1996).
[16] K.B. Efetov, Adv. Phys. **32**, 53 (1983); *Supersymmetry in Disorder and Chaos* (Cambridge University Press, Cambridge, 1997).
[17] F. Wegner, Z. Phys. B **36**, 209 (1980).
[18] M. Janssen, Phys. Rep. **295**, 1 (1998).
[19] V.E. Kravtsov and K.A. Muttalib, Phys. Rev. Lett. **79**, 1913 (1997).
[20] B.I. Shklovskii, B. Shapiro, B.R. Sears, P. Lambrianides, and H.B. Shore, Phys. Rev. B **47**, 11487 (1993).
[21] B.L. Altshuler, I.K. Zharekeshev, S.A. Kotochigova, and B.I. Shklovskii, Zh. Eksp. Teor. Fiz. **94**, 343 (1988) [Sov. Phys. JETP **67**, 625 (1988)].
[22] M. Moshe, H. Neuberger, and B. Shapiro, Phys. Rev. Lett. **73**, 1497 (1994); K.A. Muttalib, Y. Chen, M.E.H. Ismail, and V.N. Nicopoulos, Phys. Rev. Lett. **71**, 471 (1993).
[23] A.D. Mirlin, Y.V. Fyodorov, F.-M. Dittes, J. Quezada, and T.H. Seligman, Phys. Rev. E **54**, 3221 (1996).
[24] L.S. Levitov, Phys. Rev. Lett. **64**, 547 (1990).
[25] B.L. Altshuler and L.S. Levitov, Phys. Rep. **288**, 487 (1997).
[26] A.M. Garcia-Garcia, cond-mat/0309445 (2003).
[27] P.W. Anderson, Phys. Rev. **109**, 1492 (1958).
[28] G. Yeung and Y. Oono, Europhys. Lett. **4**, 1061 (1987).
[29] C.C. Yu, Phys. Rev. Lett. **63**, 1160 (1989).
[30] R. Metzler and J. Klafter, Phys. Rep. **339**, 1 (2000).
[31] F. Evers and A.D. Mirlin, Phys. Rev. Lett. **84**, 3690 (2000); E. Cuevas, M. Ortuno et.al. Phys. Rev. Lett. **88**, 016401 (2002).
[32] K. Takahashi, cond-mat/0403284 (2004).
[33] N. Mae and S. Iida, J. Phys. A **36**, 999 (2003).
[34] V.E. Kravtsov and A.D. Mirlin, JETP Lett. **60**, 656 (1994).
[35] A.M. Garcia-Garcia and J.J.M. Verbaarschot, Nucl. Phys. **B586**, 668 (2000).
[36] J.J.M. Verbaarschot and I. Zahed, Phys. Rev. Lett. **70**, 3852 (1993).
[37] A.V. Andreev, B.D. Simons, and N. Taniguchi, Nucl. Phys. B **432**, 487 (1994).
[38] V.E. Kravtsov and A.M. Tsvelik, Phys. Rev. B **62**, 9888 (2000).
[39] A. M. Garcia-Garcia and J.J.M. Verbaarshot, Phys. Rev. E **67**, 046104 (2003).
[40] F. Calogero, J. Math. Phys. **10**, 2191 (1969); B. Sutherland, J. Math. Phys. **12**, 246 (1971).
[41] A.D Mirlin, Phys. Rep. **326**, 259 (2000).
[42] A.M. Garcia-Garcia and J.C. Osborn, hep-th/0312146 (2003).
[43] J. Gasser and H. Leutwyler, Phys. Lett. **188B**, 477 (1987); Nucl. Phys. **B307**,763 (1988).
[44] M.E. Berbenni-Bitsch, M. Göckeler, T. Guhr, A.D. Jackson, J.-Z. Ma, S. Meyer, A. Schäfer, H.A. Weidenmüller, T. Wettig, and T. Wilke, Phys. Lett. B **438**, 14 (1998); M. Gockeler, H. Hehl, P.E.L. Rakow, A. Schafer, and T. Wettig, Phys. Rev. D **59**, 094503 (1999).
[45] A. Parshin and H.R. Schober, Phys. Rev. B **57**, 10232 (1998).